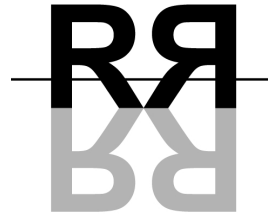




IST-2001-34744

RealReflect



D10.1: TEST REPORT ON DATA ACQUISITION

Author: Georg Zotti <gzotti@cg.tuwien.ac.at>
Institute of Computer Graphics and Algorithms, TU Vienna

Author: Vlastimil Havran <havran@mpi-sb.mpg.de>
Max-Planck-Institut fuer Informatik, Saarbruecken, Germany

Author: Attila Neumann <aneumann@cg.tuwien.ac.at>
Institute of Computer Graphics and Algorithms, TU Vienna

Version: *Revision* : 1.16 (draft)

Date: *CVS Date* : 2005/02/23 17 : 10 : 29

Abstract

This document fulfills the REALREFLECT project deliverable D10.1. In this report, we try to validate the BTF database by comparison of average colour values of the BTF images with colour values reconstructed from BRDF measurements of the same materials. A perfect match could not be achieved, however, due to the limited immediate comparability of the reference measurements it appears that the estimated error is acceptable.

Contents

1	Introduction	1
2	Colour Transformations	3
3	Coordinate System of UBO's BTF Images	5
4	Integra measurements and representation	7
4.1	BRDF format representation	7
4.2	BRDF measurements	8
5	Resampling BRDF data	11
6	Reciprocity Check	13
7	Colour Comparison	15
7.1	Preprocessing	15
7.2	Colour Difference Evaluation	17
8	Results of Color Comparison	19
	Bibliography	21

Chapter 1

Introduction

The purpose of this report is to give an answer to the question whether the BTF recording and processing instrumentation implemented by UBO is valid. To our best knowledge, such a verification has not been done yet, so we had to design our own methods of how we would proceed. Our test consist on two different manner of verification. One of them verifies plausibility of the BTF sampling in itself, and the other means a comparison of the BTF data to another set of data resulting in another sort of acquisition of the same material.

The self-verification is not obvious at all, since as it is well known, data of individual texels of a given BTF don't correspond to any BRDF, or any other texel wise separable systematic collection of data either, due to its locally unpredictable behaviour. However, averaging the data of textels by fixing their directional coordinates, a direction dependent set of data is obtained, which formally can be considered also for a BRDF. Following the derivation of *Helmoltz reciprocity* condition of BRDFs [Chand:60], we can see, that this average BTF must also fullfil it, that is the average BTF is also a BRDF not only by its dimensionality but also by its content. This statement can be seen also by the following commonsense consideration. Averaging corresponds to the same material which forms an only texel, like e.g. in mipmapping, i.e. it corresponds to magnifying its unit. All the interreflections and occlusions in which different pixels take part, distroying the pixelwise BRDF behaviour, are belonging to the same huge pixel. Therefore it still belongs to the interactions defining the BRDF of the huge pixel. The exceptional events at the border are not significant, especially after averaging their errors, that is averaging their variances.

The comparison based verification requires a different source of data, that is another technology of data acquisition. There are two important points to be recognised. Firstly, the more different technology the higher reliability of a positive result of their comparison. Secondly, a different source of data can introduce also additional altering, by other words, the more different input the more required postprocessing. This process can extend to their formal definition as well as their additional transformations.

The only available data for surface reflectivity hitherto have been BRDF data, i.e. data of uniform, spatially invariable surface reflectivity, with colour values resulting from illumination angle, viewing angle, illuminant and potential colour filter. On the other hand, BTF means bidirectional *texture* function, meaning high-frequency colour differences dependent on surface locations. The BTF samples are (processed) photographs of real materials, so they are images of some dimensions $x.y$.

Chapter 2

Colour Transformations

The first step to process the BTF samples therefore was to average each image and create a singular colour value per image. The original version of the BTF images came in BMP and JPG formats in sRGB colour space. Therefore the averaging had to take gamma into account by using the transformation

$$c' = c/12.92 \quad \text{if } c \leq 0.03928$$
$$c' = \left(\frac{c+0.055}{1.055} \right)^{2.4} \quad \text{otherwise}$$

where c is one of R, G, B and is in the range $[0...1]$.

The revised version of the UBO BTF database uses Radiance HDR format without any gamma, making averaging a strictly linear process of addition and division.

Next, these RGB values are transformed to the CIE XYZ color space:

$$\begin{pmatrix} X \\ Y \\ Z \end{pmatrix} = \begin{pmatrix} 0.4142 & 0.3576 & 0.1805 \\ 0.2126 & 0.7152 & 0.0722 \\ 0.0193 & 0.1192 & 0.9505 \end{pmatrix} \cdot \begin{pmatrix} R \\ G \\ B \end{pmatrix}$$

To compare colors and estimate a “color difference”, these XYZ values have to be transformed into a perceptually uniform color space, e.g., CIE L*a*b*. The quite elaborate conversion from CIE XYZ to CIE L*a*b*1976 can be found in the literature [EzMatch].

Chapter 3

Coordinate System of UBO's BTF Images

The BTF images have been recorded in a roughly uniform density of illumination and observation directions over the hemisphere. Deliverable D4.1 describes the setup in detail. All 4 materials investigated here were processed with the angular set H_2 described in D4.1, page 6. The available directions θ_V, θ_L were 0, 15, 30, 45, 60 and 75 degrees with different increments of the respective ϕ (azimuth) directions, see Table 3.1. However, where images could not be taken due to camera-light occlusion, a slightly different θ_L was used, which had to be taken into account for the interpolation of BRDF values. The angular values for all measurements can be seen in the tables of the accompanying document D10.1-B.

θ	15	30	45	60	75
$\Delta\phi$	60	30	20	18	15

Table 3.1: Nominal θ directions and their respective increments of ϕ .

Chapter 4

Integra measurements and representation

4.1 BRDF format representation

The following parameters are taken into account in the BRDF description (Figure 4.1):

- Spectral dimension

- Incoming ray representation:

ψ the azimuth of incidence and

σ the incident angle.

ψ is counted in the direction of the counterclockwise rotation around the normal vector.

- Outgoing ray representation:

θ the angle between the directions of specular reflected and observation directions.

ϕ the angle between the incidence plane and the plane coinciding with the observation and specular reflection directions.

ϕ is counted in the direction of the counterclockwise rotation around the specular reflected ray.

The data is presented as a table with values defined in nodes and values between nodes linearly interpolated. The type of BRDF data color model can be RGB or spectral; in the later case wavelength (WL) coefficients define falling illumination transformed according to BRDF.

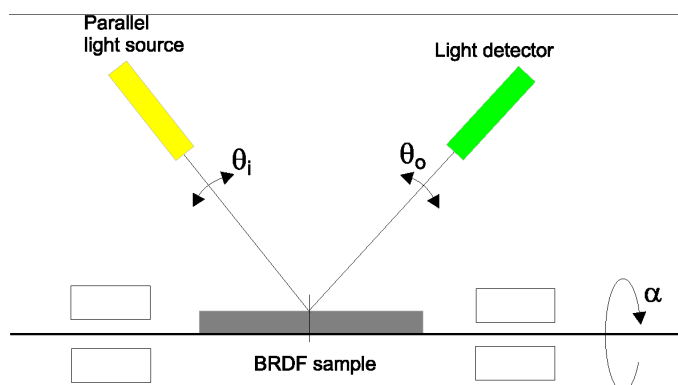


Figure 4.1: Parametrization of the integra representation.

4.2 BRDF measurements

BRDF is measured twice, separately for a specular and for diffuse component. For the sample materials we obtained, the diffuse component was measured only. Three of the four sample materials were not specular enough to use the device for a specular component.

The main elements of the device are:

- illuminating system forming a narrow parallel beam of light
- detector which registers light reflected by sample
- standard diffusor

The diffuse component of BRDF is a complex angular function that depends on incidence and observation directions. Therefore, the equipment must provide measurements inside of the 2π solid angle above/under the sample (Figure 4.2). It is achieved by

1. rotation of the light source in the plane of drawing (incident angle θ_i);
2. rotation of the detector (reception angle θ_o) and
3. rotation of the sample (inclination angle α).

The measurement for the same lighting and observation conditions are executed two times: first for the sample, and then for a perfect standard diffusor. The relation between the luminance of the sample and the perfect diffusor is the *Luminance Factor* for specific lighting and observation conditions.

BRDF data depend on the wavelength of illuminating light. Different equipment can be applied to provide spectral measurements. For example, a monochromator with a dispersive element (prism, diffraction grating, etc.) or a set of lasers emitting light of different wavelength.

The Integra format allows to specify efficiently various types of BRDFs. The four samples measured exhibit plane symmetry formed by isotropic surfaces. Scattering depends on angle of incidence and direction of outgoing ray, it does not depend on the azimuth angle of incident ray

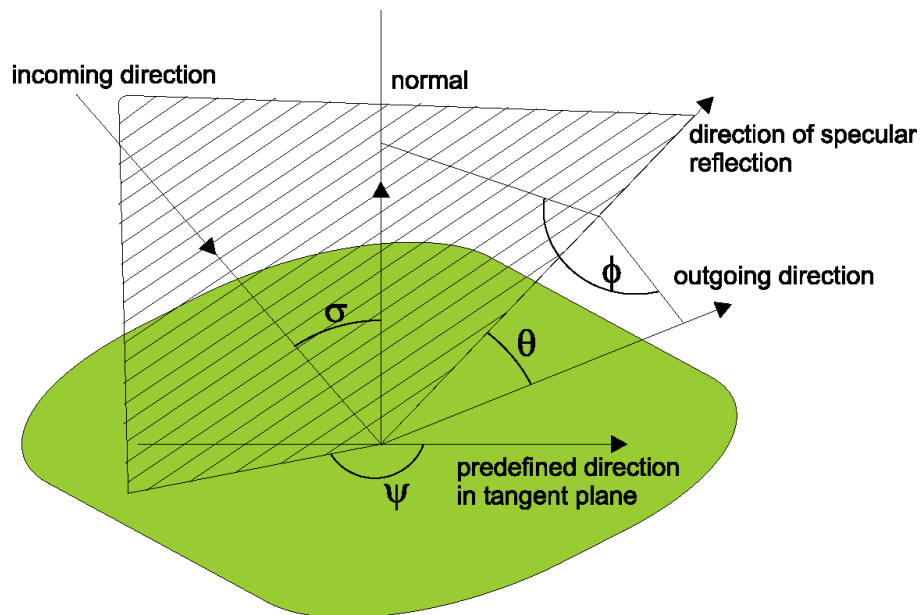


Figure 4.2: Gauge setup for measurements of diffuse BRDF by Integra

(so it describes a 3D BRDF). This type of BRDF has plane symmetry, where the symmetry plane contains incident ray and surface normal. That is why the range of definition ϕ is $0 \leq \phi < 180^\circ$.

The measurements by Integra are provided in the data files for incoming angles $\theta_i \in \{0, 10, 20, 30, 45, 60, 90\}$.

Chapter 5

Resampling BRDF data

The BRDF measurements represent the function in 3D space by set of sample points with associated function values. The measurements in the first setting result in the set of samples that is different from the set of samples of the second measurement. In order to compare the two measurements of the same reality at the set of the discrete points, we have to resample the first function from one set of points to the reference set of points of the second function. Similarly, we can resample the second function to the set of points given by the first function, which is not studied here but should be described in a forthcoming paper.

Our sample data are highly irregular, especially the samples measured by Integra. Since BRDFs are isotropic, the resampling actually occurs in 3D space in general. However, the subset of incoming θ angles is covered well in both domains: 0, 30, 45, and 60 degrees. For these data the interpolation is performed only in 2D space.

For the interpolation properties the continuity of the function support with respect to the geometrical setting is highly important. Traditional hemispherical parametrization θ, ϕ is not suitable, since there is a strong discontinuity for $\phi = 0$ and the mapping from a square is highly non-linear along the pole ($\theta = 0$). For this reason we remapped the direction to a 2D square using the mapping proposed by Shirley [Shirley:97][Shirley:92], which keeps fractional surface area from 2D to 3D. In addition it has the nice property that it is continuous around the pole with respect to the input variables x and y , which is a necessary property for correct interpolation at this region.

Although there are various interpolation and extrapolation schemes, for example *Radial Basis Functions*, we have chosen Shepard's method for 2D and 3D data, since they work according to our experiments acceptably. We also tested the RBF interpolation scheme in both global and local setting. However, the results of RBF interpolation from highly irregular (Integra) data were worse than for Shepard's interpolation scheme. For the survey of the interpolation techniques see [Franke:99], [Lodha:99]. In particular, we use the method by Renka for 2D data [Renka88a] [Renka99].

Chapter 6

Reciprocity Check

The principal idea of BRDF as *Bidirectional Reflection Distribution Function* is the exchangeability of view and light directions: the colour of a surface point should not change if lightsource and eye directions are exchanged. (Of course, changing light distance would make a difference!) Given that diffuse surface brightness is largely dependent on the cosine of the angle θ_L between illumination direction and surface normal, a colour value for normal incidence can be reconstructed by dividing each colour component by $\cos\theta_L$. Now, for pairs with $\theta_{V1} = \theta_{L2}, \phi_{V1} = \phi_{L2}, \theta_{L1} = \theta_{V2}, \phi_{L1} = \phi_{V2}$, a relation like $(XYZ)_1 / \cos\theta_{L1} = (XYZ)_2 / \cos\theta_{L2}$ should hold for perfect diffuse surfaces.

During reciprocity check, CIE XYZ and L values have been compared to estimate colour differences. Table 6.1 shows the maximum differences as results.

The validation run over the original version of the BTF database (top 4 rows), performed in February 2004, showed significant shortcomings at this stage, making further validation work pointless, and required UBO to re-process all BTF data, which was finished by October 2004. The new data in HDR format were similarly processed, the results are shown in the lower half of Table 6.1. While still recognizable, these errors are much less and should be in practice acceptable. Also, perfect reciprocity could not be expected due to phenomena occurring in rough materials, like 3D microstructure, subsurface light transport, interreflections, etc.

Material	θ_{V1}	ϕ_{V1}	θ_{L1}	ϕ_{L1}	$ X_2 - X_1 $	$ Y_2 - Y_1 $	$ Z_2 - Z_1 $
ceiling_panel	45	260	75	225	40.31852	6.01261	13.30624
floortile	45	280	75	0	19.09562	2.21568	7.47488
floor_plastic	75	105	75	270	13.58390	1.78117	13.28481
glazed_tile	75	15	75	330	32.40578	2.07974	10.50744
ceiling_panel_hdr	45	260	75	225	5.39506	5.75663	5.19840
floortile_hdr	75	75	75	240	2.20551	2.32750	2.34216
floor_plastic_hdr	75	105	75	270	3.18606	3.39167	3.60704
glazed_tile_hdr	75	15	75	330	9.80880	10.34563	10.00222

Table 6.1: Colour differences occurring during reciprocity tests.

Chapter 7

Colour Comparison

Motto: “What you can compare, compare. What you cannot compare, make it comparable.”

7.1 Preprocessing

The BTF data provided by UBO lack absolute albedo values, which prohibit a direct comparison with the Atrium BRDF data. But, given that only 3-channel colour values (RGB, or CIE XYZ derivable from RGB) are available which can be matched, the following idea can be applied.

If colour values v for the same directions as used in the BTF acquisition can be created from the BRDF in a linear colour space, e.g., CIE XYZ, there is a linear transformation between each respective pair v, w of colour triplets, where v resembles the colour produced from the processing of the BRDF data with an assumed white illuminant like D65, and w the average colour of a BTF photograph.

This transformation can be expressed as 3×3 matrix T so that

$$\begin{pmatrix} t_{11} & t_{12} & t_{13} \\ t_{21} & t_{22} & t_{23} \\ t_{31} & t_{32} & t_{33} \end{pmatrix} \cdot \begin{pmatrix} v_1 \\ v_2 \\ v_3 \end{pmatrix} = \begin{pmatrix} w_1 \\ w_2 \\ w_3 \end{pmatrix} \quad (7.1)$$

Theoretically, the same matrix T should be found by all i equations for the i corresponding color samples. In practice, this cannot be expected, but to find a meaningful solution a common T can be derived from the given 6561 corresponding pairs i of colour values, which can transform the colour values with the smallest error. This matrix can be found by means of a least-squares fitting method.

We have to minimize the function $F = \sum_i (T \cdot v^{(i)} - w^{(i)})^2$, where $v^{(i)}$ is the i -th entry of set v , which corresponds to the equation system $\frac{\partial F}{\partial t_{kl}} = 0$ ($k = 1 \dots 3, l = 1 \dots 3$), since the function F is convex with a single minimum point. In addition, we may want to introduce weighting factors a_k for the 3 individual colour channels k to emphasize the importance of, say, the Y channel by introducing a *weighted dot product*, $x \odot y = \sum a_k x_k y_k$ which corresponds to the weighted norm $\|x\| = \sum a_k x_k^2$. We have

$$\begin{aligned}
 F &= \sum_i (T \cdot v^{(i)} - w^{(i)}) \odot (T \cdot v^{(i)} - w^{(i)}) \\
 &= \sum_i ((T \cdot v^{(i)}) \odot (T \cdot v^{(i)}) + w^{(i)} \odot w^{(i)} - 2(T \cdot v^{(i)}) \odot w^{(i)}) \\
 &= \sum_i \left(\sum_{k=1}^3 a_k (T \cdot v^{(i)})_k^2 + \sum_{k=1}^3 a_k w_k^{(i)2} - 2 \sum_{k=1}^3 a_k (T \cdot v^{(i)})_k w_k^{(i)} \right) \\
 &= \sum_i \sum_{k=1}^3 (a_k (T \cdot v^{(i)})_k^2 + a_k w_k^{(i)2} - 2a_k (T \cdot v^{(i)})_k w_k^{(i)})
 \end{aligned}$$

Now, $(T \cdot v)_k = t^{(k)} \cdot v = \sum_{l=1}^3 t_{kl} v_l = t_{k1} v_1 + t_{k2} v_2 + t_{k3} v_3$, so $\frac{\partial (T \cdot v)_k}{\partial t_{kl}} = v_l$ ($k = 1 \dots 3, l = 1 \dots 3$), and we obtain 9 equations to solve ($k = 1 \dots 3, l = 1 \dots 3$):

$$\begin{aligned}
 0 &= \frac{\partial F}{\partial t_{kl}} = \sum_i \left(2a_k (T \cdot v^{(i)})_k \cdot \frac{\partial (T \cdot v^{(i)})_k}{\partial t_{kl}} - 2a_k \frac{\partial (T \cdot v^{(i)})_k}{\partial t_{kl}} \cdot w_k^{(i)} \right) \\
 &= 2a_k \sum_i \left(\sum_{m=1}^3 (t_{km} \cdot v_m^{(i)}) v_l^{(i)} - v_l^{(i)} \cdot w_k^{(i)} \right)
 \end{aligned}$$

Obviously, factor $2a_k$ can be omitted from further consideration, which points out surprisingly that the solution is generic for weights (a_1, a_2, a_3) , that is, independent from any weighting of the channels, and we look for a zero point of the derivative:

$$Eq_{k,l} : \frac{1}{2a_k} \frac{\partial F}{\partial t_{kl}} = 0 : \sum_{m=1}^3 t_{km} \sum_i v_m^{(i)} v_l^{(i)} = \sum_i v_l^{(i)} w_k^{(i)}$$

We see that we have now 3 separate equation systems for $k = 1, 2, 3$ surprisingly with the *same* 3×3 core matrix $A : A_{lm} = \sum_i v_m^{(i)} v_l^{(i)}$, ($l = 1 \dots 3, m = 1 \dots 3$), which is a symmetric matrix. Simplifying our notations ($k = 1 \dots 3$):

$$\begin{aligned}
 T &= \begin{pmatrix} t^{(1)} \\ t^{(2)} \\ t^{(3)} \end{pmatrix} \quad \text{with} \\
 t^{(k)} &= (t_{k1}, t_{k2}, t_{k3}) \quad \text{and} \\
 b^{(k)} &= \left(\sum_i v_1^{(i)} w_k^{(i)}, \sum_i v_2^{(i)} w_k^{(i)}, \sum_i v_3^{(i)} w_k^{(i)} \right)
 \end{aligned}$$

we can write each 3-variable equation ($k = 1 \dots 3$) with solution, where e.g. $t^{(k)T}$ is the transposed (column vector form) of $t^{(k)}$, as

$$A t^{(k)T} = b^{(k)T}$$

and, because A is symmetric,

$$\begin{aligned} t^{(k)}A &= b^{(k)} \\ t^{(k)} &= b^{(k)}A^{-1} \end{aligned}$$

and with

$$B = \begin{pmatrix} b^{(1)} \\ b^{(2)} \\ b^{(3)} \end{pmatrix} \quad (7.2)$$

we can write

$$T = BA^{-1} \quad (7.3)$$

The matrices T thus obtained are:

$$T_{\text{ceiling_panel}} = \begin{pmatrix} 3.207 & -1.406 & -1.144 \\ 3.404 & -1.486 & -1.218 \\ 3.461 & -1.578 & -1.196 \end{pmatrix} \quad (7.4)$$

$$T_{\text{floortile}} = \begin{pmatrix} 0.875 & 1.174 & -1.568 \\ 0.912 & 1.255 & -1.659 \\ 0.994 & 1.197 & -1.675 \end{pmatrix} \quad (7.5)$$

$$T_{\text{floor_plastic}} = \begin{pmatrix} 2.671 & -0.664 & -1.614 \\ 2.797 & -0.684 & -1.699 \\ 2.324 & -0.370 & -1.575 \end{pmatrix} \quad (7.6)$$

$$T_{\text{glazed_tile}} = \begin{pmatrix} -0.357 & 0.954 & -0.226 \\ -0.377 & 1.007 & -0.238 \\ -0.339 & 0.965 & -0.245 \end{pmatrix} \quad (7.7)$$

7.2 Colour Difference Evaluation

Now that we have a best average transformation matrix between the colour sets, we can transform the colour values v of the colours computed from the reference BRDF and can then finally compare the two sets $T \cdot v, w$ in a meaningful way. The CIE and other experts of colour science provided numerous functions for colour comparison over the last decades [EzMatch], which take into account not absolute values of (re)radiation, but also the colour sensitivity of the human visual system, which means that the numerical results represent validity in terms of detectability with the human visual system.

In this work we use the CIE Lab 1976 set of colour differences, DC notates *Chroma Difference*. In addition, we give the newer *CIELAB2000 total colour difference* DEexp. We give average and median values in Table 8.1.

Chapter 8

Results of Color Comparison

In these tables, a colour difference value of 1 means “barely detectable”. As can be seen from average and median values, the error is usually very small. The floor plastic material is rough on a larger scale, so here self-shadowing of bumps is evident in the images and leads to greater average differences between the two data sets.

Material	Metric	max	avg	med
ceiling_panel_hdr	DE	34.0932	2.5867	2.0099
	DEexp	31.0316	2.2277	1.6820
floortile_hdr	DE	65.3709	3.9574	2.2777
	DEexp	60.2893	3.5386	1.9823
floor_plastic_hdr	DE	102.2380	6.7738	4.8795
	DEexp	75.3385	5.7009	3.9840
glazed_tile_hdr	DE	95.6749	8.0871	6.1314
	DEexp	68.0128	6.9738	5.2866

Table 8.1: Colour differences occurring during colour comparison tests. The full tables are given in the supplement document D10.1-B.

Investigating the full tables explains the reason for the high maximum values: These occur exactly for directions where $\theta_V = \theta_L$ and $\phi_V = \phi_L + 180$, which means looking into the exact direction of specular reflection. Given that the Integra BRDF data describe only the diffuse component of the reflective behaviour, while the BTF images include diffuse and specular reflections, large deviations had to be expected at these directions. Also, extrapolating colour values from the BRDF at points with extreme specularities will yield greater errors. On the other side, in the respective images of the original series, some amount of detector burnout was apparent. With the new HDR format, the exceedingly high values for specular reflection can be properly represented. The on-screen appearance for the user has then to be properly processed in the tonemapping stage.

All in all, the resulting differences are well inside the range expected from the uncertainties present in the original data.

Bibliography

- [AtriumSite] MPI. *Atrium Website*. <<http://www.mpi-sb.mpg.de/resources/atrium/brdfdata.html>> (as of 11/2004).
- [Ba91] HANS-JOCHEN BARTSCH. *Taschenbuch Mathematischer Formeln*. Fachbuchverlag Leipzig (1991).
- [Chand:60] S CHANDRASHEKHAR. *Radiative Transfer*. Dover Publication Inc, New York (1960).
- [EzMatch] HUNTER LAB. *EasyMatch Textiles Manual, Ch.28*. <<http://www.hunterlab.com/kb/software/eztexvalues.pdf>> (visited 02/2004).
- [Franke:99] R. FRANKE. *Scattered data interpolation: tests of some methods*. Math. Comp., 38, pp.181–199 (1982).
- [Lodha:99] S. K. LODHA AND R. FRANKE. *Scattered Data Techniques for Surfaces*. In: H. Hagen, G. Nielson and F. Post (eds.), Proceedings of Dagstuhl Conference on Scientific Visualization, pp.182–222, IEEE Computer Society Press (1999).
- [Renka88a] ROBERT J. RENKA. *Multivariate interpolation of large sets of scattered data*. In: ACM Trans. Math. Softw., 14(2), pp.139–148, ACM Press, ISSN 0098-3500 (1988).
- [Renka88b] ROBERT J. RENKA. *ALGORITHM 661: QSHEP3D: quadratic Shepard method for trivariate interpolation of scattered data*. In: ACM Trans. Math. Softw., 14(2), pp.151–152, ACM Press, ISSN 0098-3500 (1988).
- [Renka99] ROBERT J. RENKA. *Algorithm 790: CSHEP2D: cubic Shepard method for bivariate interpolation of scattered data*. In: ACM Trans. Math. Softw., 25(1), pp.70–73, ACM Press, ISSN 0098-3500 (1999).
- [Shirley:92] P. SHIRLEY. *Nonuniform Random Point Sets via Warping*. In: D. Kirk (ed.), Graphics Gems III, pp.80–83, Academic Press, San Diego (1992).
- [Shirley:97] P. SHIRLEY AND K. CHIU. *A Low Distortion Map Between Disk and Square*. In: Journal of Graphics Tools, 2(3), pp.45–52 (1997).

